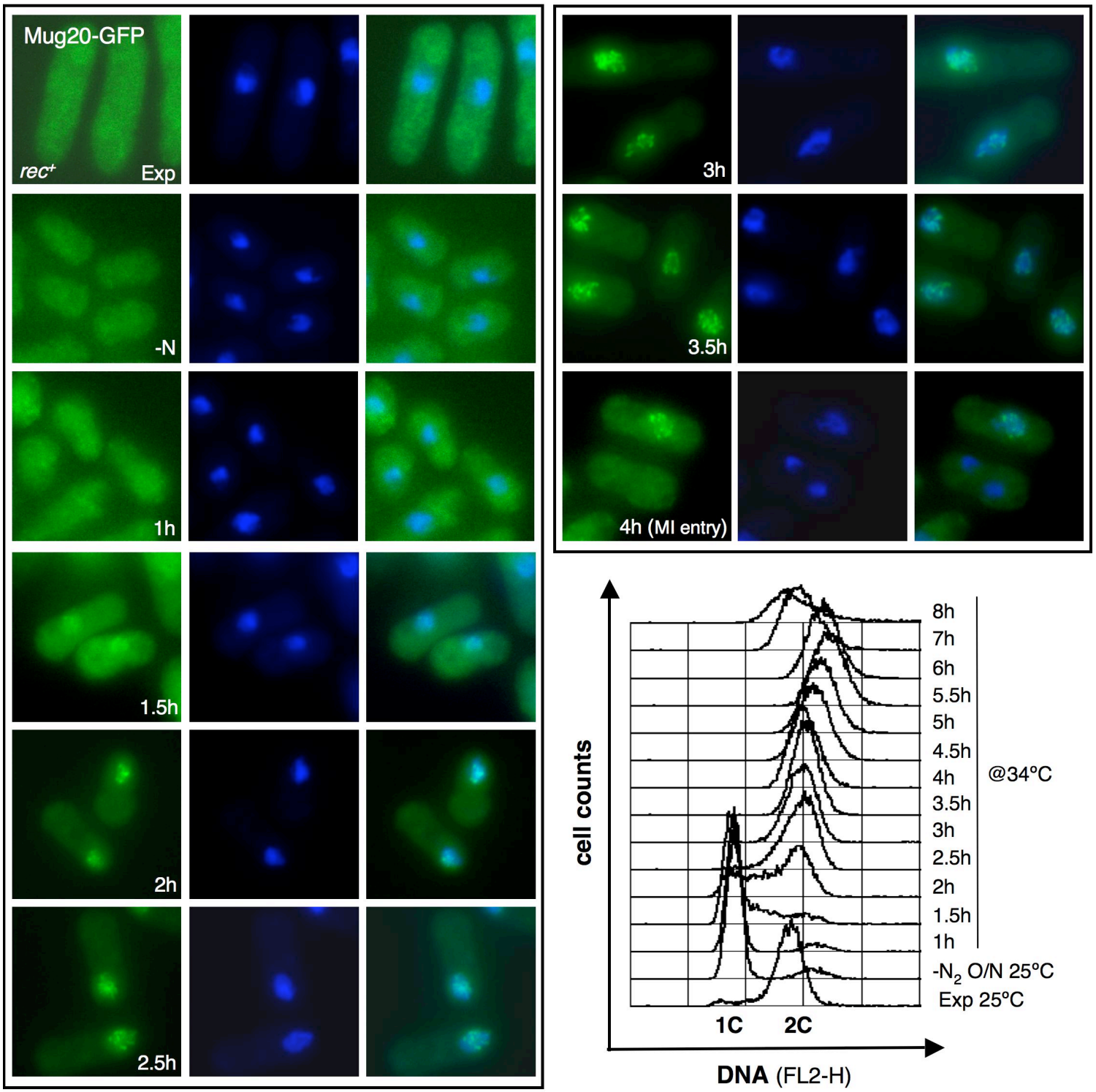

Figure S1. Time course of localization of Mug20-GFP (related to Figure 2). Cells were synchronously induced for meiosis, fixed, and examined at the times indicated by fluorescence microscopy for GFP foci (left panels), DNA (DAPI-staining; middle panels), and both (merge; right panels). The lower right panel shows flow cytometry data for DNA replication. Note that in all cases foci are prominent from 2.5 hr (shortly after the completion of replication) to 4 hr (beginning of MI; unpublished data). Conditions for these experiments produced meiotic events about 0.5 hr earlier than the conditions for the ChIP-chip analyses at 3.5 hr for most of the data shown here; this time is when LinE signals were maximal.

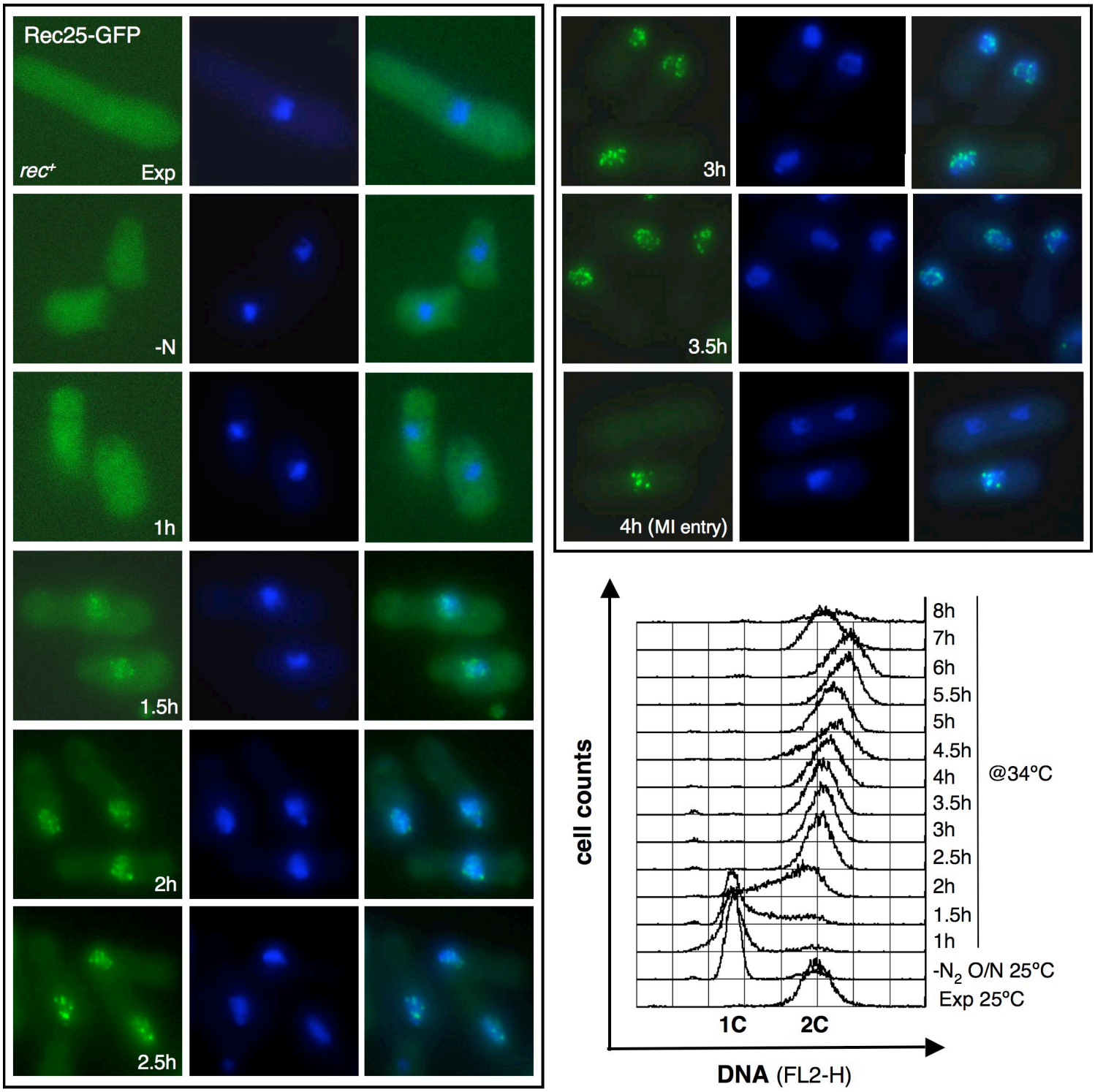

Figure S2. Time course of localization of Rec25-GFP (related to Figure 2). Cells were synchronously induced for meiosis, fixed, and examined at the times indicated by fluorescence microscopy for GFP foci (left panels), DNA (DAPI-staining; middle panels), and both (merge; right panels). The lower right panel shows flow cytometry data for DNA replication. Note that in all cases foci are prominent from 2.5 hr (shortly after the completion of replication) to 4 hr (beginning of MI; unpublished data). Conditions for these experiments produced meiotic events about 0.5 hr earlier than the conditions for the ChIP-chip analyses at 3.5 hr for most of the data shown here; this time is when LinE signals were maximal.

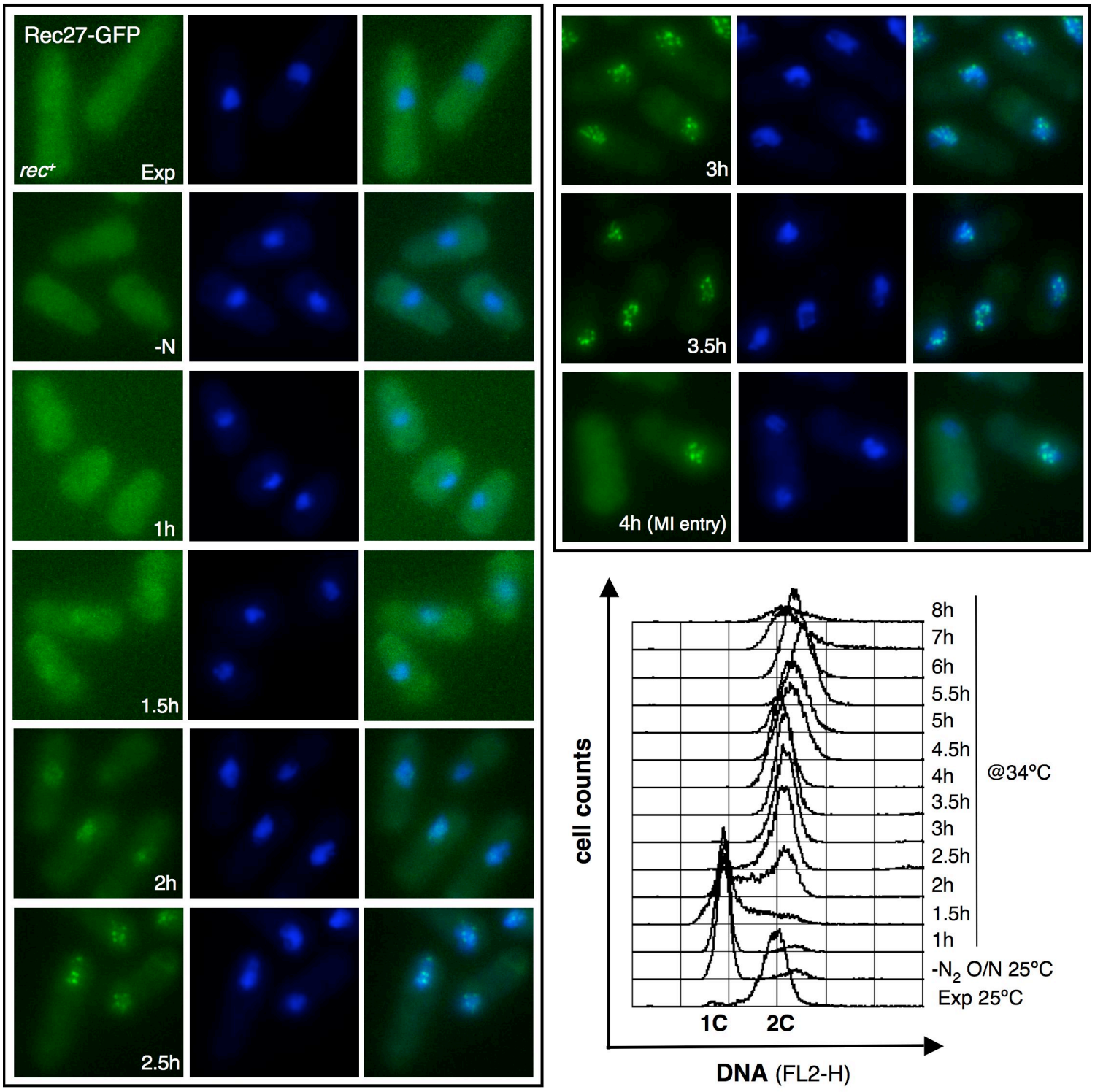

Figure S3. Time course of localization of Rec27-GFP (related to Figure 2). Cells were synchronously induced for meiosis, fixed, and examined at the times indicated by fluorescence microscopy for GFP foci (left panels), DNA (DAPI-staining; middle panels), and both (merge; right panels). The lower right panel shows flow cytometry data for DNA replication. Note that in all cases foci are prominent from 2.5 hr (shortly after the completion of replication) to 4 hr (beginning of MI; unpublished data). Conditions for these experiments produced meiotic events about 0.5 hr earlier than the conditions for the ChIP-chip analyses at 3.5 hr for most of the data shown here; this time is when LinE signals were maximal.

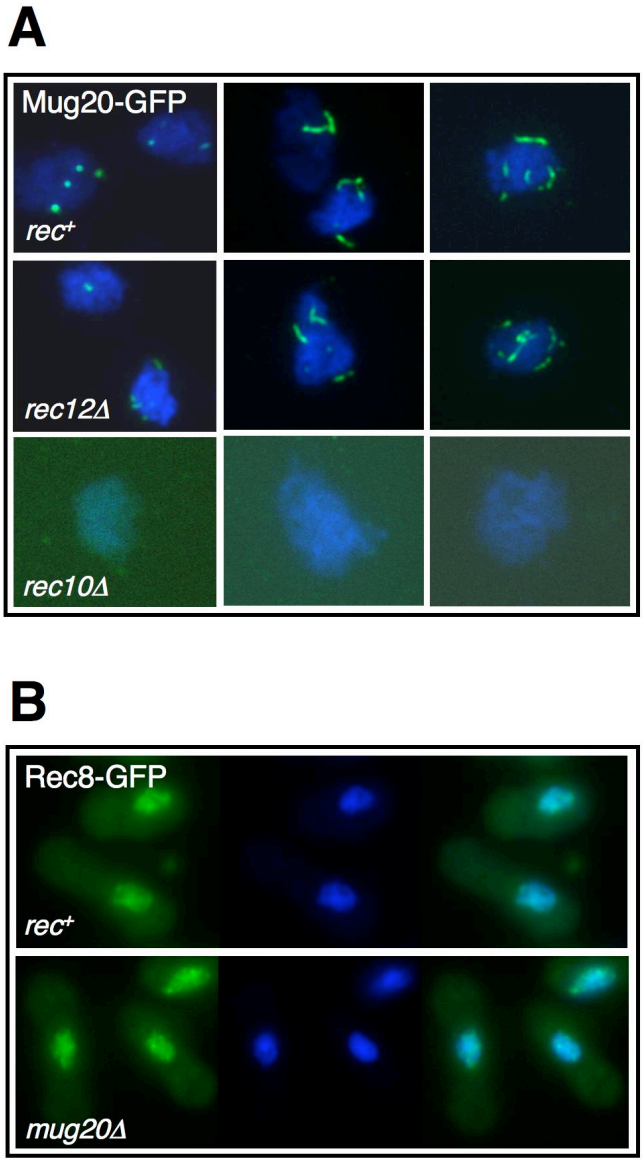

Figure S4. Focus-formation by Mug20-GFP and Rec8-GFP (related to Figure 2). (A) Mug20-GFP forms foci in nuclear spreads in the absence of DSB-formation (in rec12Δ) but not in the absence of Rec10. Nuclear spreads from paraformaldehyde-fixed spheroplasts (Davis et al., 2008) were prepared at 2 hr (left image), 2.5 hr (middle), or 3 hr (right) after meiotic induction; merged GFP and DAPI-stained images are shown. (B) Rec8 forms nuclear foci in intact cells even in the absence of Mug20. Cells were fixed 3 hr after meiotic induction and stained with DAPI.

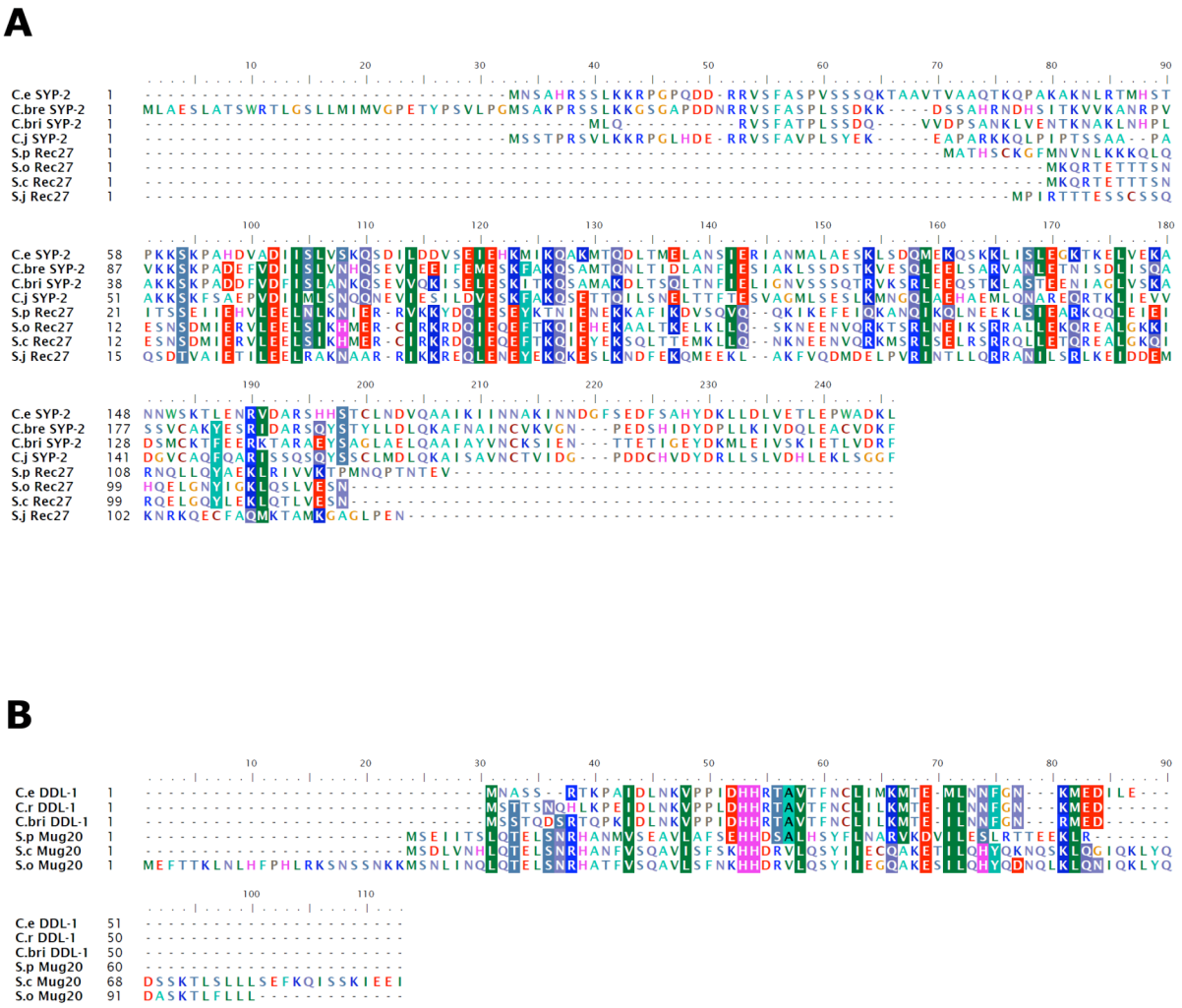

Figure S5. Similarity in amino acid sequences of *S. pombe* Rec27 and Mug20 and those of *C. elegans* SYP-2 and Ddl-1 (related to Figure 1).
Amino acid sequences were aligned and plotted with BioEdit using ClustalW (gap open penalty, 10; gap extend penalty, 0.2). The BLOSUM62 (BLocks SUbstitution Matrix) was used to color residues with similar physicochemical properties. Shaded blocks indicate positions where at least two thirds of sequences agree. The putative coiled-coil domains of Mug20 and Ddl-1 have been removed, because they forced alignment to themselves and obscured the alignment of the N-terminus shown here. *Caenorhabditis* species are abbreviated as follows: C.e, *C. elegans*; C.bre, *C. brenneri*; C.bri, *C. briggsae*; C.j, *C. japonica*; C.r, *C. remanei*. *Schizosaccharomyces* species are similarly abbreviated: S.p, *S. pombe*; S.o, *S. octosporus*; S.c, *S. cryophilus*; S.j, *S. japonicus*.

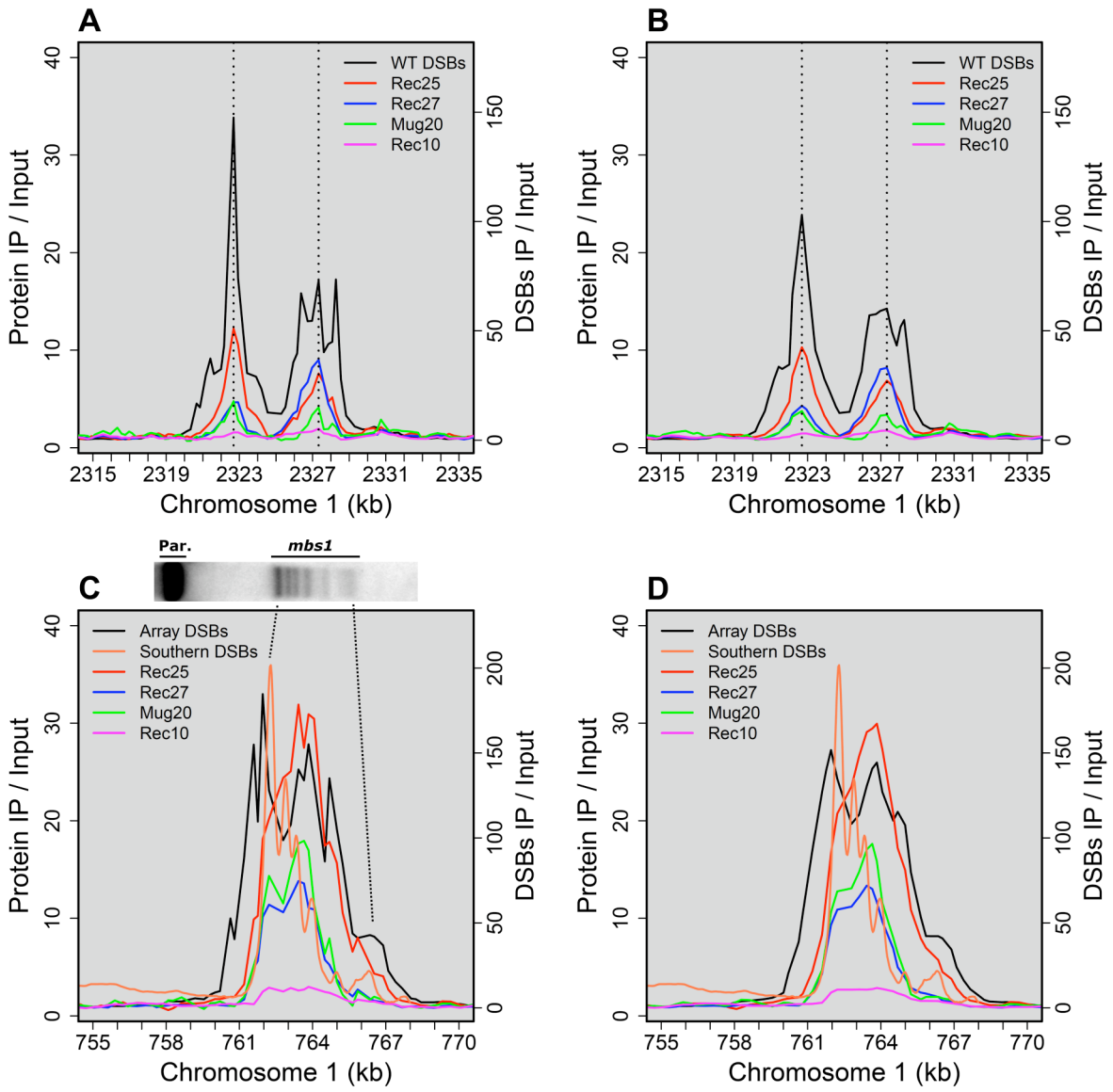

Figure S6. High resolution views of DSB and protein distribution at DSB hotspots (related to Figure 3A).
(A) DSBs and binding of four LinE proteins to two hotspots, about 5 kb apart, near the middle of chromosome 1. Dotted lines are at the center of the most prominent DSB signal. Note that the most prominent protein binding signals are ≤0.5 kb from this line, indicating that the resolution of these data is <1 kb. **(B)** Data of Figure S6A smoothed with an 11-probe (~3 kb) window. **(C)** DSBs and binding of four LinE proteins at the *mbs1* hotspot near the left end of chromosome 1. A tracing of DSBs determined by Southern blot hybridization and Phosporimage analysis (orange line) is superimposed on the ChIP-chip data. DNA extracted at 5 hr after meiotic induction of strain GP2958 was digested with *Mlu*I and analyzed for DSBs with a probe at the right end of the 20.9 kb *Mlu*I fragment (Young et al., 2002). The tracing was adjusted for the log-linear nature of DNA migration using markers on the same gel and aligned by the positions of the *Mlu*I sites at 748600 and 769529 bp. See Figure 3A for description. **(D)** ChIP-chip data smoothed with an 11-probe (~3 kb) window and Southern blot trace of Figure S6C.

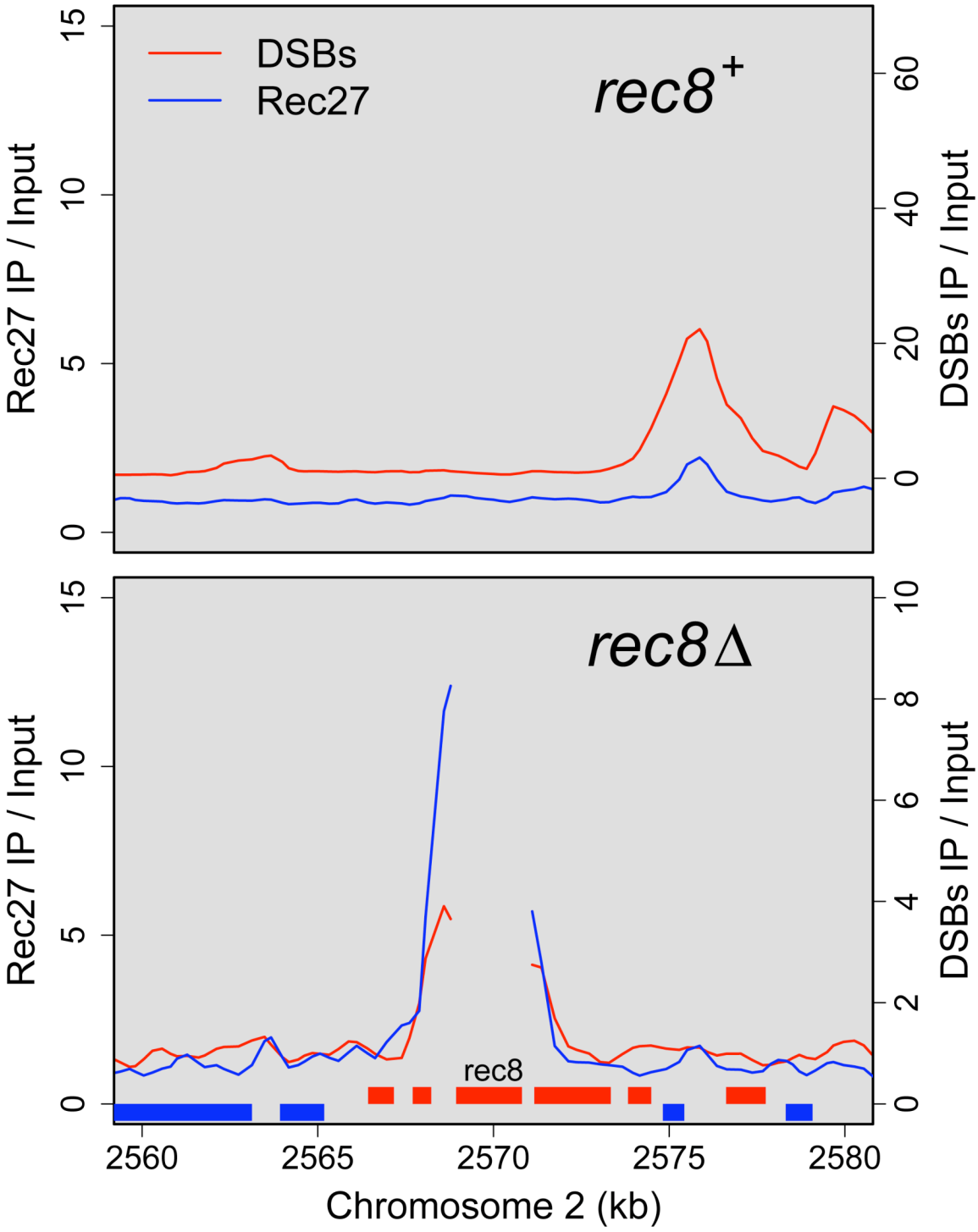

Figure S7. Insertion of exogenous DNA creates a DSB hotspot and a Rec27 binding site (related to Figure 3D). Shown is the *rec8* locus from wild type (top) and from *rec8::kanMX6* deletion (bottom; missing probes are those of the deletion). In wild type the *rec8* locus is cold for both DSBs and Rec27 binding, but an intergenic region about 5 kb to the right is moderately hot for both. In *rec8::kanMX6* this locus is moderately hot for both, and the region to the right has become cold.

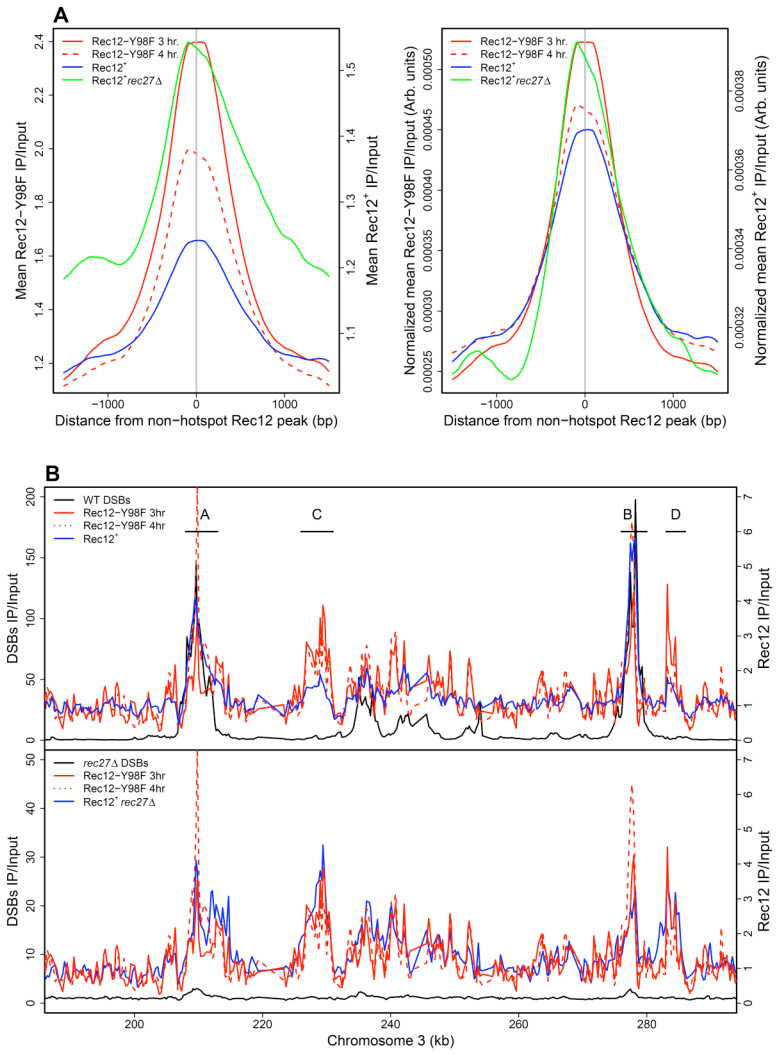

Figure S8. Rec12 and the inactive Rec12-213(Y98F) proteins bind across the genome similarly, including at sites with little or no DSB formation, in the presence or absence of Rec27 (related to Figure 3).

(A) Immunoprecipitates of sonicated chromatin from cells harvested after synchronous induction of meiosis were analyzed as in Figure 3 for DNA crosslinked with formaldehyde to Rec12^{+} (at 3.5 hr after meiotic induction, in *rec27*$^{+}$ and in *rec27Δ*) and Rec12-213(Y98F) (one experiment at 3 hr and one at 4 hr). The binding values (median normalized IP/WCE) around each of the 223 most prominent low-level Rec12-213(Y98F) 3 hr peaks were aligned at their centers and the mean values of those data to each side of the center were plotted; peaks were defined as sites where at least two consecutive probes were enriched a minimum of 2-fold over genome median. Data for the other determinations were plotted using the centers of the Rec12-213(Y98F) 3 hr peaks as the basis. Similar results were obtained when the 4 hr Rec12-213(Y98F) data were used as the basis. Sites within the 288 DSB hotspots (see supplemental methods) were excluded since, for the proficient Rec12, this could reflect low-level Rec12 self-linkage and obscure the Rec12 binding profile. The data were graphed without normalization (left panel) or after normalizing each site to the site's total signal to correct for large peaks biasing the spatial pattern (right panel). Note that the data for Rec12-213(Y98F) are similar for the 3 and 4 hr analyses; this result supports the 3.5 hr analyses for most of the assays reported here being representative of this period of meiosis. Note also that the centers, heights, and widths of the curves are similar for all determinations; this result suggests that the two proteins bind similarly and that Rec12^{+} binds similarly in the presence or absence of Rec27.

(B) (Top) Data from a section of chromosome 3 were median-normalized and plotted without smoothing or an offset. Note that sites A and B have abundant DSBs and Rec12 binding, and that sites C and D have negligible DSBs but abundant Rec12 binding which is nevertheless similar in Rec12 and Rec12-213(Y98F). (Bottom) As in top panel but DSBs (Rec12^{+} self-linkage) and Rec12^{+} crosslinked with formaldehyde in a *rec27Δ* strain; Rec12-213(Y98F) data are re-plotted for comparison. Data for the whole genome are on the Lab Websites.

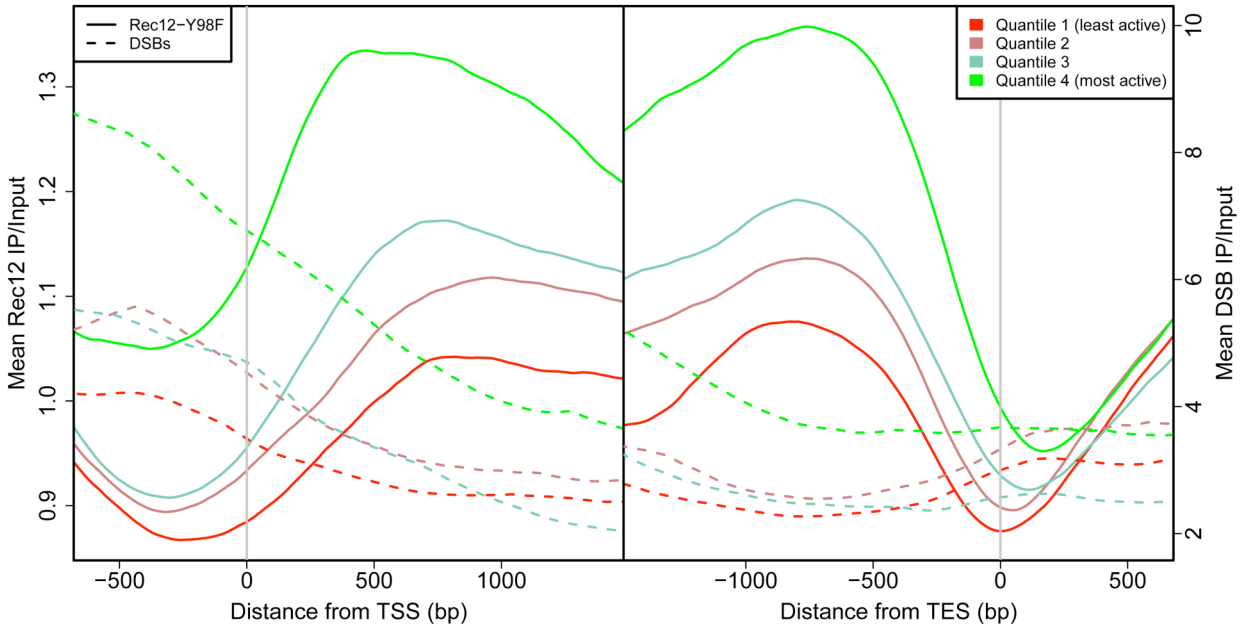

Figure S9. Evidence that transcription influences the binding of Rec12 and DSB-formation (related to Figure 6B).

The degree of binding of Rec12-213(Y98F) (formaldehyde crosslinked) at 4 hr and frequency of DSBs (Rec12 self-linkage) were averaged as in Figure S8A. The median normalized data (IP/WCE) were aligned at the beginning (TSS) and end (TES) of each annotated transcriptional unit for which we had meiotic expression data. Genes were arranged according to the abundance of transcripts at 4 hr of meiosis (Chen et al., 2012). Data for each quartile of genes, from least abundant to most abundant transcripts, were averaged and plotted. Note that for each gene set DSBs are less abundant within genes than in the immediate region 5' of the gene, but the converse is true for Rec12 binding. Note also that the differential between within-gene and outside-of-gene increases with increasing transcript abundance, as does the absolute mean signal; this result indicates that a higher level of transcription strongly increases Rec12 binding but has less effect on DSB formation within genes. Furthermore, Rec12-213(Y98F) binding, but not DSBs, is strongly defined by the TSS and TES.